Research Article

Erick José Torres-Martínez, Ricardo Vera-Graziano, José Manuel Cervantes-Uc, Nina Bogdanchikova, Amelia Olivas-Sarabia, Ricardo Valdez-Castro, Aracely Serrano-Medina, Ana Leticia Iglesias, Graciela Lizeth Pérez-González, José Manuel Cornejo-Bravo*, and Luis Jesús Villarreal-Gómez*

Preparation and characterization of electrospun fibrous scaffolds of either PVA or PVP for fast release of sildenafil citrate

https://doi.org/10.1515/epoly-2020-0070
received March 28, 2020; accepted June 18, 2020

Abstract: Sildenafil citrate (SC) has proved to be an effective and inexpensive drug for the treatment of pulmonary arterial hypertension (PAH). This study aims to synthesize electrospun, submicron fiber scaffolds of poly(vinyl alcohol) (PVA) and poly(vinyl pyrrolidone) (PVP) loaded with SC for fast drug dissolution and its potential use in the treatment of PAH. These fiber scaffolds were prepared through the electrospinning technique. The chemical composition of the nanofibers was analyzed by Fourier transform infrared spectroscopy. Thermal stability was studied by thermogravimetric analysis and polymeric transitions by differential scattering calorimetry. Surface analysis of the nanofibers was studied by field emission scanning electron microscopy. The wetting and dissolution time of the scaffolds and drug release rate were studied as well. The drug-loaded PVP fibers showed better quality regarding size and homogeneity compared to drug-loaded PVA fibers. These fibers encapsulated approximately 2.5 mg/cm^2 of the drug and achieved immediate controlled released rate, which is encouraging for further studies leading to an alternative treatment of PAH in children.

Keywords: fibrous scaffolds, electrospinning, sildenafil citrate, poly(vinyl alcohol), poly(vinyl pyrrolidone)

*** Corresponding author: José Manuel Cornejo-Bravo,** Universidad Autónoma de Baja California, Calzada Universidad 14418, Parque Industrial Internacional, Tijuana, Baja California C.P. 22390, México; Facultad de Ciencias Químicas e Ingeniería, Universidad Autónoma de Baja California, Unidad Otay, Tijuana, Baja California, México, e-mail: jmcornejo@uabc.edu.mx, tel: +52-664-676-8222
*** Corresponding author: Luis Jesús Villarreal-Gómez,** Universidad Autónoma de Baja California, Calzada Universidad 14418, Parque Industrial Internacional, Tijuana, Baja California C.P. 22390, México; Facultad de Ciencias Químicas e Ingeniería, Universidad Autónoma de Baja California, Unidad Otay, Tijuana, Baja California, México; Facultad de Ciencias de la Ingeniería y Tecnología, Universidad Autónoma de Baja California, Unidad Valle de las Palmas, Tijuana, Baja California, México, e-mail: luis.villarreal@uabc.edu.mx, tel: +52-664-676-8222
Erick José Torres-Martínez, Graciela Lizeth Pérez-González: Universidad Autónoma de Baja California, Calzada Universidad 14418, Parque Industrial Internacional, Tijuana, Baja California C.P. 22390, México; Facultad de Ciencias Químicas e Ingeniería, Universidad Autónoma de Baja California, Unidad Otay, Tijuana, Baja California, México; Facultad de Ciencias de la Ingeniería y Tecnología, Universidad Autónoma de Baja California, Unidad Valle de las Palmas, Tijuana, Baja California, México
Ricardo Vera-Graziano: Instituto de Investigaciones en Materiales, Universidad Nacional Autónoma de México, Ciudad de México, México
José Manuel Cervantes-Uc: Centro de Investigación Científica de Yucatán, A.C., Mérida, Yucatán, México
Nina Bogdanchikova, Amelia Olivas-Sarabia, Ricardo Valdez-Castro: Centro de Nanociencias y Nanotecnología, Universidad Nacional Autónoma de México, Ensenada, Baja California, México
Aracely Serrano-Medina: Universidad Autónoma de Baja California, Calzada Universidad 14418, Parque Industrial Internacional, Tijuana, Baja California C.P. 22390, México; Facultad de Medicina y Psicología, Universidad Autónoma de Baja California, Unidad Otay, Tijuana, Baja California, México
Ana Leticia Iglesias: Universidad Autónoma de Baja California, Calzada Universidad 14418, Parque Industrial Internacional, Tijuana, Baja California C.P. 22390, México; Facultad de Ciencias de la Ingeniería y Tecnología, Universidad Autónoma de Baja California, Unidad Valle de las Palmas, Tijuana, Baja California, México
ORCID: José Manuel Cornejo-Bravo 0000-0002-0013-8937; Luis Jesús Villarreal-Gómez 0000-0002-4666-1408

1 Introduction

Pulmonary arterial hypertension (PAH) is a common complication of congenital heart disease (CHD). This condition is a progressive disorder characterized by high blood pressure in the pulmonary artery (1). CHD is the most frequent birth defect, with a prevalence ranging from 6 to 8 per 1,000 live births. Unfortunately, this disease has high mortality and morbidity rates (2). Several therapies are used to treat PAH; however, sildenafil citrate (SC) is one of the most cost-efficient treatments (3). This drug inhibits phosphodiesterase 5 (PDE5) by blocking its catalytic site, which prevents the degradation of the cyclic guanosine monophosphate molecule, promoting vascular smooth muscle relaxation and increased blood flow, thus relieving the symptoms of PAH. SC was approved for PAH treatment in children by the Food and Drug Administration (FDA) and the European Medicines Agency in 2005 (4).

However, there are no commercial presentations of the drug for pediatric patients (5). For instance, some hospitals administer SC as an extemporaneous syrup prepared using the powder produced by grounding SC tablets, just before administrating it to patients. This approach, besides being tedious and time-consuming, may be associated with the administration of incorrect doses. Moreover, there is a real concern about the stability of the drug in aqueous solutions (2). Thus, there is a need to develop stable formulations for SC that can be administered to children. Our approach is to develop fast-dissolving SC-loaded nanofiber scaffolds for rapid dissolution in oral mucosa, taking advantage of the efficient absorption of drugs in the mouth because of the high vascularization in the sublingual zone (5).

The electrospinning technique is a promising approach to fabricate efficient drug delivery systems. This method is used to produce fibers with diameters ranging from sub-nanometers to several micrometers. These fibers can be formed using polymers, metals, ceramics, and composite materials, which makes this technique quite versatile (6). Electrospun drug delivery systems have better control and predictability on drug delivery than the conventional systems. Moreover, nanofiber scaffolds possess high surface-to-volume ratio, which can accelerate the dissolution of drugs in aqueous media and improve their bioavailability (6–11).

Poly(vinyl alcohol) (PVA) has been widely used in the pharmaceutical industry because of its versatile properties such as high hydrophilicity, biocompatibility, and suitable thermal properties, among others (7). Moreover, PVA is an interesting polymer for drug delivery because of its electrospinnability and mucoadhesive properties (8). Another well-studied polymer for electrospinning is poly(vinyl pyrrolidone) (PVP), which has been reported to exhibit good properties as complexing, adhesion, physiological compatibility, low chemical toxicity, and reasonable solubility in water and most organic solvents. Therefore, it has a wide range of industrial applications such as pharmaceutical, cosmetics, beverages, adhesives, detergents, paints, electronic materials, and bioengineering (9). In addition, PVP is more commonly used to assist the formation of nanofibers from inorganic materials (9). PVP also absorbs up to 40% of its weight in water, what makes it a good matrix for the solid dispersion of poorly soluble drugs (10).

Notwithstanding the fact that there are a great number of reports about electrospun nanofibers used as carriers of pharmaceutical drugs (6), to the best of our knowledge, this is the first report about SC loaded into electrospun nanofibers for fast controlled release. In this study, we prepared and characterized SC-loaded submicron fiber scaffolds using two polymeric materials as matrixes: PVA and PVP. Therefore, the objective of this work is to formulate a delivery system for the rapid dissolution and its potential use in the treatment of PAH in children. This study includes the evaluation of the physicochemical properties of both the controls and the drug-loaded formulations. Finally, drug release from these fiber scaffolds was studied.

2 Material and methods

2.1 Materials

The materials used in this study are PVA (Product #: 341584, CAS: 9002-89-5, Sigma Aldrich, MW: 89,000 to 98,000 mol wt, hydrolysis of 98–99%) and PVP 40 (Product #: PVP40, CAS: 9003-39-8, Sigma-Aldrich, MW: 40,000 mol wt). Other materials used such as deionized water (H_2O) (Product #: 38796, CAS: 7732-18-5), ethanol (EtOH) (≥99.5%, Product #: 459844, CAS: 64-17-5), Triton™ X-100 (TX-100) (Product #: X100-500 mL, CAS: 0009002931), and *N*,*N*-dimethylformamide (DMF), anhydrous (99.8%, Product #: 227056) were also from Sigma-Aldrich; all were used as received. SC 99% was kindly

donated by SBL Pharmaceuticals S.L de R. L., Baja California, México.

2.2 Preparation of drug-loaded scaffolds

The standard technique of mixing the therapeutic agent with polymer solutions before electrospinning remains the most predominant technique to prepare drug-loaded submicron fiber scaffolds (6). Therefore, such technique was tested to prepare SC-loaded polymeric solutions for the fabrication of the functionalized fibers.

For the PVA fiber scaffolds, a 10% (w/v) solution of PVA was prepared using a H_2O:DMF mixture as solvent (Table 1). The solutions were placed in an 80°C water bath with constant stirring (200 rpm), until a homogeneous solution was obtained. The prepared solutions were settled at 3°C overnight to remove any bubbles. After that, 2 µL of TX-100 was added to reduce the surface tension for PVA electrospinning at 20 kV (10).

For the PVA/SC nanofibers scaffolds, the pharmaceutical drug was dissolved in a mixture of H_2O and DMF (Table 1). The latter was added to increase the conductivity as well as a co-solvent for SC, as the drug has low water solubility (4.1 mg/mL), compared to DMF with a solubility of 10 mg/mL. Moreover, different proportions of the co-solvents were tested to achieve good dissolution of the polymer and the drug, as well as adequate electrospinning conditions (Table 1). Constant magnetic stirring (200 rpm) and heat were applied until dissolution (80°C). Subsequently, the polymer was added to obtain a concentration of 10% (w/v) and stirred until a homogeneous solution was formed. Finally, 2 µL TX-100 was added to the solutions to break down the surface tension of the polymeric solution.

A similar procedure was followed for the preparation of PVP solutions. In this case, 30% w/v PVP solutions were prepared in different proportions of absolute ethanol and DMF. As previously, DMF was added to increase the conductivity as well as a co-solvent for SC, because it also has low solubility in ethanol (10). In this case, there was no need for the use of a surfactant to achieve the formation of the fibers. The conditions of the solutions that could be electrospun are described in Table 1.

Table 1: Formulations of drug-loaded polymeric solutions

Sample code	PVA conc. (% w/v)	SC conc. (% w/v)	Solvent mixture (A/B/C) (v/v)
PVA/SC0	10	0	84/15/1
PVA/SC1	10	1.25	84/15/1
PVA/SC2	10	2.5	84/15/1
PVA/SC3	10	5	79/20/1
Sample code	**PVP conc. (% w/v)**	**SC conc. (% w/v)**	**Solvent mixture (D/B) (v/v)**
PVP/SC0	30	0	85/15
PVP/SC1	30	1.25	85/15
PVP/SC2	30	2.5	75/25
PVP/SC3	30	5	70/30

PVA: poly(vinyl alcohol); PVP: poly(vinyl pyrrolidone); SC: sildenafil citrate. Solvents: (A) H_2O: distilled water; (B) DMF: *N*,*N*-dimethylformamide; (C) TX-100: Triton X-100; (D) EtOH: ethanol.

2.3 Electrospinning process

For fiber scaffolds formation, the following procedure was performed: 3 mL of PVA/SC or PVP/SC solutions were loaded to a plastic syringe (needle tip of 22G). Then, the distances from the needle tip to the collector was set at 10 cm for PVA and 15 cm for PVP, respectively. For both polymeric solutions, 20 kV and 0.5 mL/h flow rate were applied. Experiments were conducted at ~25°C and 30% of relative humidity (environmental parameters were fixed with the lab thermostat and drierite desiccants [W A Hammond Drierites CO]).

2.4 Characterization of PVP and PVA fibrous scaffolds

2.4.1 Spectroscopic characterization by ATR-FTIR

The infrared attenuated total reflectance (ATR) spectra were obtained with a Fourier transform infrared spectrophotometer (Thermo Scientific Nicolet IS5). Spectral data were collected at 20°C, in the range of 4,000–650 cm^{-1}, using a high-performance diamond ATR crystal. Thirty-two scans were performed at a resolution of 4 cm^{-1}. To process the data, the OMNIC™ Specta Software (Thermo Scientific) was used.

2.4.2 Field emission scanning electron microscopy

The morphology and diameter of the prepared fibers were determined by field emission scanning electron microscopy (FESEM) under an accelerating voltage of 20 kV, using small sections of fibrous material (field emission microscope JEOL JSM 7600F).

2.4.2.1 Determination of the average fiber diameter and porosity

Software Image J was used to measure the fiber diameter and the percentage of pore area in the membranes. SEM images of 10,000× for the pure PVA and 5,000× for the rest of the samples were used for this purpose. Thirty fields were used for the calculation of fiber diameters and scaffold-porosity ratio.

2.4.3 Thermal behavior analysis (thermogravimetric analysis and differential scanning calorimetry)

2.4.3.1 Thermogravimetric analysis

Thermogravimetric analysis (TGA) was performed by measuring the change of mass as temperature increases. The tests were carried out using a heating rate of 10°C/min from room temperature (±20°C) to 400°C in an unsealed platinum sampler using nitrogen with a flow rate of 20 mL/min. The equipment used was a Shimadzu model TGA-Q500. The mass of the samples analyzed varied between 5 and 10 mg. This technique allowed us to determine the temperature at which thermal degradation begins (T_{onset}) and the change in mass per temperature increase. The curves derived from TGA (derivative thermogravimetry [DRTG]) were generated to identify the maximum degradation temperature ($T_{deg\ max}$). TA Instruments™ software was used for the identification of temperatures.

2.4.3.2 Differential scanning calorimetry

Thermal transitions were characterized by differential scanning calorimetry (DSC) equipment Shimadzu model DSC-Q100, programmed to heat from room temperature (±20°C) to 400°C at a heat rate of 10°C/min (first run), with an argon gas flow of 20 mL/min. The mass of the samples analyzed varied between 5 and 10 mg. TA Instruments™ software was used for the identification of the temperatures.

2.4.4 Wetting and dissolution of fibers

Dissolution of the fiber scaffolds was tested according to Li et al. (11), where samples were submerged in a flask with 250 mL of distilled water at 37°C and measured as a function of time. Two layers of absorbent paper were placed in a Petri dish with a diameter of 10 cm. After the paper was completely soaked with distilled water, the excess water was completely drained. Fibrous scaffolds were placed on the moistened paper and video was recorded until complete mat dissolution. The latter was done to measure the fiber dissolution in real-time. The degradation rate was recorded with a video camera (Canon PC1304 semi-professional), mounted on a special device that controls lighting conditions to clearly observe the dissolution of the fibers. Experiments were performed in triplicate.

2.4.5 *In vitro* release study

The electrospun fibers were recovered carefully from the aluminum foil collector and weighed exactly using a digital balance (25 mg). Each sample was immersed in a flask with 40 mL of methanol/water solution (50:50), under magnetic stirring at 200 rpm for 5 min at 37°C. At appropriate time intervals 3 mL of the supernatant was extracted, and an equal volume of solvent was added to the release system to keep the volume constant during the experiment. The withdrawn samples were filtered using 0.22 µm regenerated cellulose filters, and then the concentration of extracted SC was determined by UV-Vis at 290 nm. The loading of the nanofiber was calculated from the SC dissolved after 6 h in dissolution media.

2.4.6 Statistical analysis

The experiments were performed in a threefold independent manner with internal triplicates. The results were expressed as mean ± standard deviation of three independent experiments. Data were evaluated by one-way analysis of variance (one-way ANOVA), using Graph Pad Prism version 6.0c software. The results were considered statistically significant when $p < 0.05$.

3 Results

3.1 Spectroscopic characterization by ATR-FTIR

FTIR was used to identify the characteristic signal of SC present in the polymeric samples. All signals were compared using FTIR spectrum reported by Pavia et al. (12). Figure 1a shows the FTIR spectra for the PVA/SC fibers. A distinctive peak of the O–H stretch vibration in PVA can be observed at 3,400–3,200 cm^{-1}; around 2,900 cm^{-1}, a signal characteristic to alkyl C–H stretching is visible, and

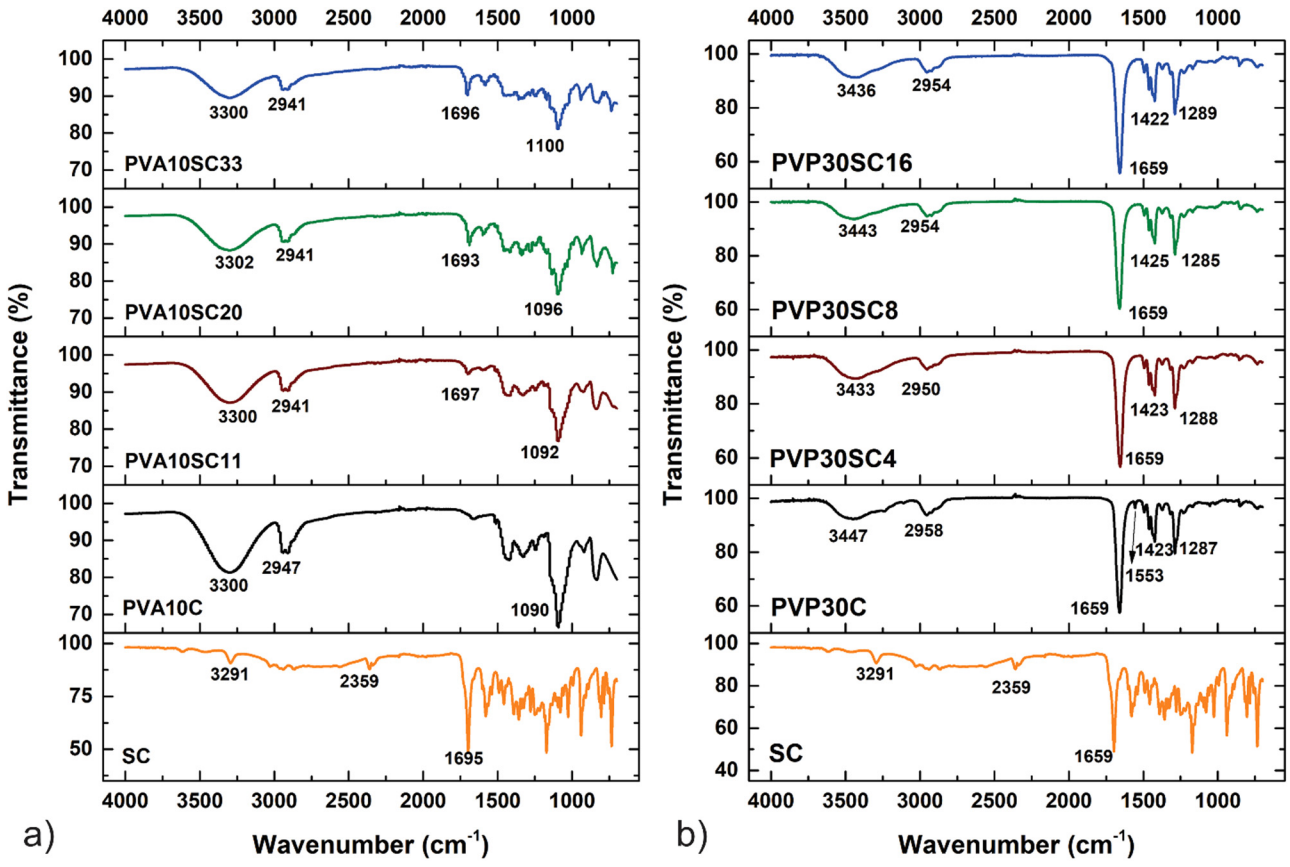

Figure 1: FTIR spectra comparison of PVA/SC and PVP/SC fibrous scaffolds. (a) PVA/SC fibers, and SC spectra; (b) PVP/SC fibers and SC spectra.

between 1,150 and 1,050 cm^{-1} a signal that corresponds to the C–O link can be observed. The PVA/SC samples show a weak signal around 1,695 cm^{-1} characteristic of carbonyl groups present in the structure of the drug.

The FTIR spectra for PVP/SC fibers are shown in Figure 1b. The PVP/SC0 sample presented a wide peak at 3,447 cm^{-1} corresponding to an overtone of C–O groups in the polymeric chains, another at 2,958 cm^{-1} attributed to alkyl C–H stretching signal, and a characteristic peak at 1,659 cm^{-1} corresponding to the carbonyl group. Stretching at 1,423 cm^{-1} is the C–H bending vibrations, and the signal at 1,285 cm^{-1} is linked to the C–N vibration.

3.2 Morphology by scanning electron microscopy (FESEM)

As it can be observed in Figures 2 and 3, all scaffolds are made of long fibers, disposed randomly on the surface to the collector.

The apparent diameter, shape, surface texture, and porosity ratio of the polymer fibers were determined by FESEM, and the micrographs were analyzed using Image J software (13) (https://imagej.nih.gov/ij/) that allowed the determination of the average fiber diameter and porosity ratio of the scaffolds through the measure of 30 fibers for each sample. The mean diameter, porosity ratio, standard deviation, median, etc. are shown in Table 2.

Comparing the average fiber diameter, it can be observed that most of them possess an approximated diameter of 450 nm, with the exception of PVA/SC0 and PVA/SC1 membranes. PVA/SC0 presented considerably thinner fibers, some in the nanometric scale (~100 nm). In contrast, PVA/SC1 showed the presence of thicker fibers (628 ± 250 nm). For PVA/SC fibers, a linear relationship between concentration of SC and diameters can be observed; increasing the amount of SC resulted in the reduction of diameters. On the contrary, for PVA fibers, including the control, the amount of SC had no effect on fiber diameter. The statistical analysis confirms the reproducibility of the electrospinning technique used in this

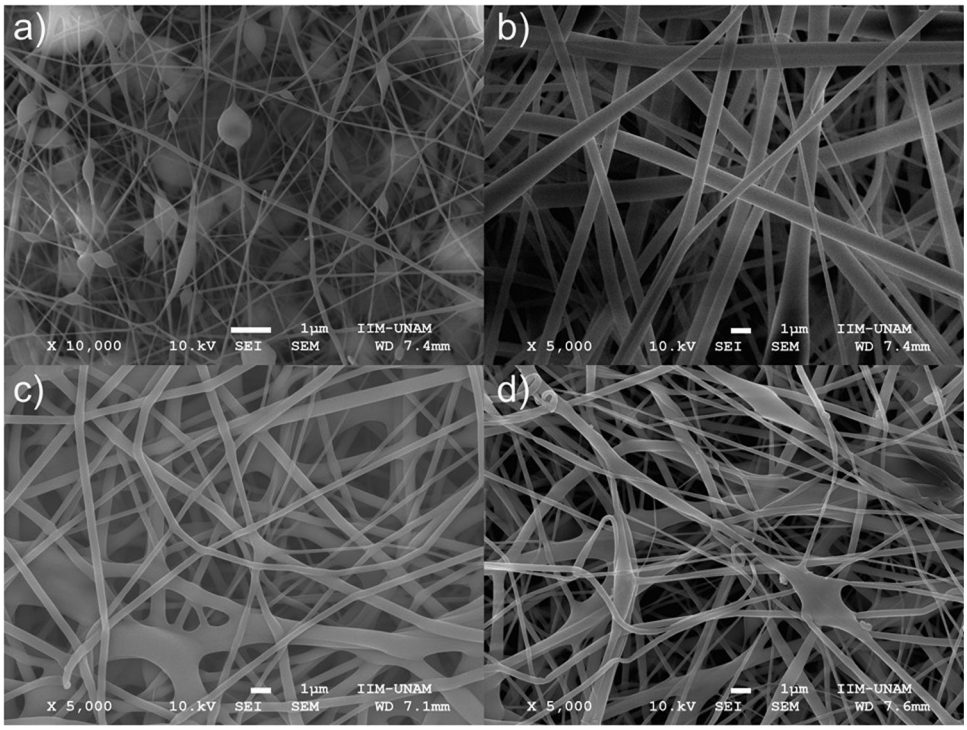

Figure 2: SEM micrographs of PVA/SC fibrous scaffolds. (a) PVA/SC0 (10,000×); (b) PVA/SC1 (5,000×); (c) PVA/SC2 (5,000×); and (d) PVA/SC3 (5,000×).

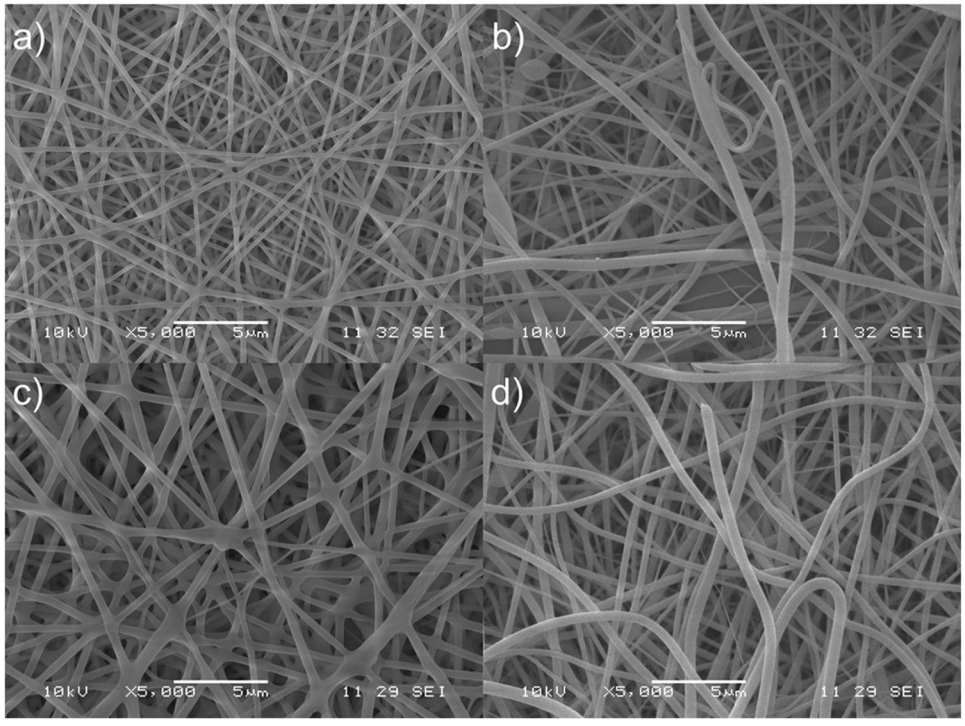

Figure 3: SEM micrographs of PVP/SC fibrous scaffolds. (a) PVP/SC0 (5,000×); (b) PVP/SC1 (5,000×); (c) PVP/SC2 (5,000×); and (d) PVP/SC3 (5,000×).

study. No significant difference (ANOVA $P < 0.05$) was found in fiber diameter between both types of polymer samples (Table 2).

In the case of porosity, all fibrous scaffolds yield similar results; mean porosity was around ~40%, apart from the PVA/SC0, which presented an ~60% mean porosity. The reproducibility observed in this parameter for all polymer types and the concentrations of SC (ANOVA $P < 0.05$) is relevant because of its relation with the dissolution rate of SC, which is pursued to be fast in both systems.

A non-ionic surfactant (TX-100) was needed for the electrospinning of all PVA fiber scaffolds to reduce the surface tension and promote reproducible results (14). In Figure 2a, the presence of bulbs along unloaded PVA/SC0 fibers can be observed, even in thin fibers (~100 nm) prepared with TX-100. In contrast, as shown in Figure 2b–d, the fibers with SC are smoother but thicker. All micrographs were taken at 5,000× of amplification.

In the case of PVP/SC0, the observed thicknesses of the fibers (Figure 3) was similar to those reported in the literature (15). The morphology of PVP/SC fibers is smooth, with more homogeneous diameter than those of PVA/SC fibers; no bulbs were found, even in the PVP/SC0 control fibers.

Finally, comparing both types of polymer fibers, those made of PVP/SC scaffolds presented better morphology and more reproducibility than PVA/SC fibers, in terms of percentage of porosity of the scaffolds, average diameter of fibers, and morphology, which are the important parameters for controlling the drug release rate and the mechanical properties of the final system (16).

Table 2: Average fiber diameter and percentage porosity ratio of PVA/SC and PVP/SC fibrous scaffolds

Samples	Average diameter ($\bar{x} \pm \sigma$) (nm)	Porosity (%)
PVA/SC0 (a)	103 ± 31	60
PVA/SC1 (b)	628 ± 250	45
PVA/SC2 (c)	481 ± 142	44
PVA/SC3 (d)	423 ± 146	42
PVP/SC0 (a)	371 ± 128	44
PVP/SC1 (b)	452 ± 144	49
PVP/SC2 (c)	402 ± 89	42
PVP/SC3 (d)	411 ± 142	41

$\bar{x}$ = average; σ = standard deviation.

3.3 Thermal behavior by TGA and DSC

The influence of SC on both thermal stability and thermal transitions on all polymer scaffolds was studied by both TGA and DSC (17).

The stability as a function of temperature of PVA/SC scaffolds is shown in Figure 4a and b. PVA/SC scaffolds show no loss of mass below ~190–200°C, meaning thermal stability, a valuable property for future biomedical applications because the scaffolds are quite stable at environmental temperatures and could be sterilized by heat. Then, between ~202°C and ~245°C an initial loss of 5% mass is observed because of the removal of solvent residues (18). The TGA curves show a second loss of mass

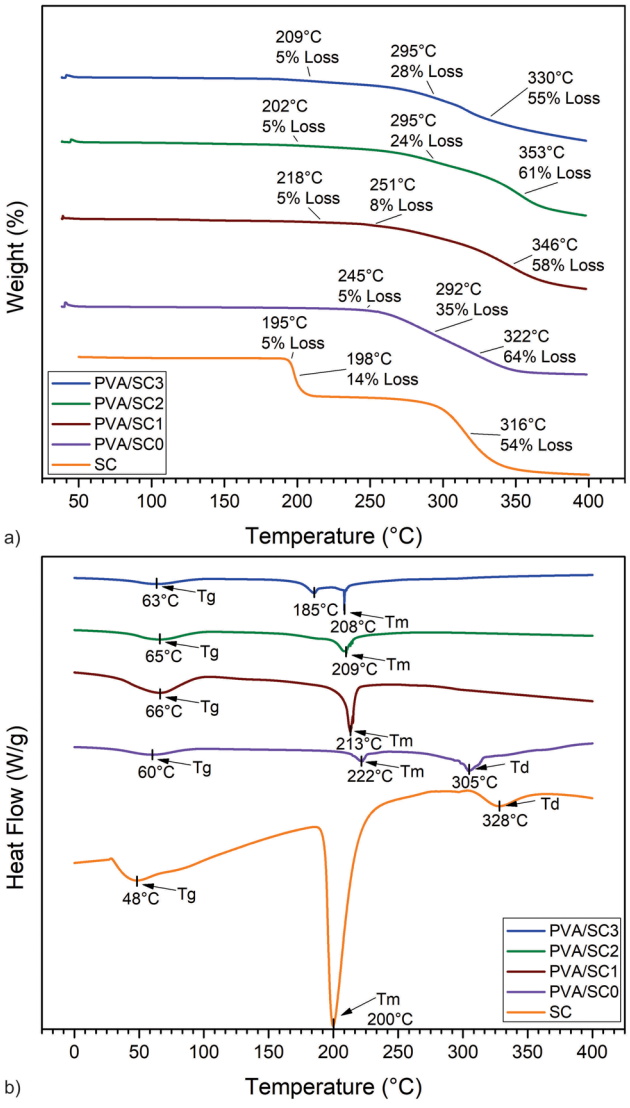

Figure 4: Thermal analysis of PVA/SC fibers. (a) TGA; (b) DSC.

starting around 245°C, another change in slope of the curves at around ~292°C is, best depicted in the first derivative curves, DTG, and a third change around 320°C. TGA and DTG curves for PVA/SC0 curves have two distinct peaks at ~292°C and ~322°C that are associated with the decomposition of side chains of PVA and the generation of volatile residues of the polymer (19). About 14% mass loss is observed in the TGA and DTG curves, at ~195–198°C (20). This transition is attributed to both removal of residual moisture and partial decomposition of the citrate component. Then, a second transition at ~316°C refers to the decomposition of the entire citric and part of the sildenafil components (20). The decomposition temperatures of all PVA/SC samples were shifted to higher temperatures with respect to PVAc sample.

The DSC curves for PVA/SC scaffolds are presented in Figure 4c. PVA/SC0 fibers showed a T_g at ~60°C, and T_g's of PVA/SC samples slightly shifted, having a maximum between ~62°C and 66°C, depending on the SC concentration. This may be because of the interaction between PVA and SC (19). Two other endothermic peaks are observed in PVA/SC0, one at ~222°C and the other reaching its mayor value at ~305°C (DSC). The first one refers to the T_m of the polymer crystalline domains, and the second peak corresponds to the decomposition temperature (T_d) of PVA (20). For the SC, a T_m was observed at ~200°C, which represents the melting point; this may range by a bit because of the presence of different polymorphs of the drug. The second peak (T_d) at ~328°C refers to the decomposition temperature of the SC (20). The melting point of SC is not present in PVA/SC1 and PVA/SC2 showing that the drug is dispersed in the matrix. Moreover, T_g values of PVA/SC fibrous mats were displaced to higher temperatures with respect to PVA/SC0 fibrous scaffolds, thus indicating the interaction between the PVA and SC molecules. PVA/SC3 presents a small endothermic peak at ~185°C, indicating possible drug aggregation in the nanofibers.

Figure 5a and b shows the thermal behavior of PVP and PVP/SC fibers. For the PVP/SC0 sample, the TGA curve shows an initial drop of 5% between ~30°C and ~254°C, corresponding to the removal of moisture. For the PVP/SC0 scaffolds, above ~350°C the polymer mass starts to decay because of its decomposition at high temperatures (21). For the PVP/SC, a higher weight loss occurs at 255°C, compared to the loss of pure PVP at this temperature.

The DSC curves are shown in Figure 5c. Again, pristine SC presents the T_m at ~200°C and the decomposition of the drug at ~328°C (20). The T_g's of the PVP/SC samples occur almost near the T_g of PVP/SC0, but as the concentration

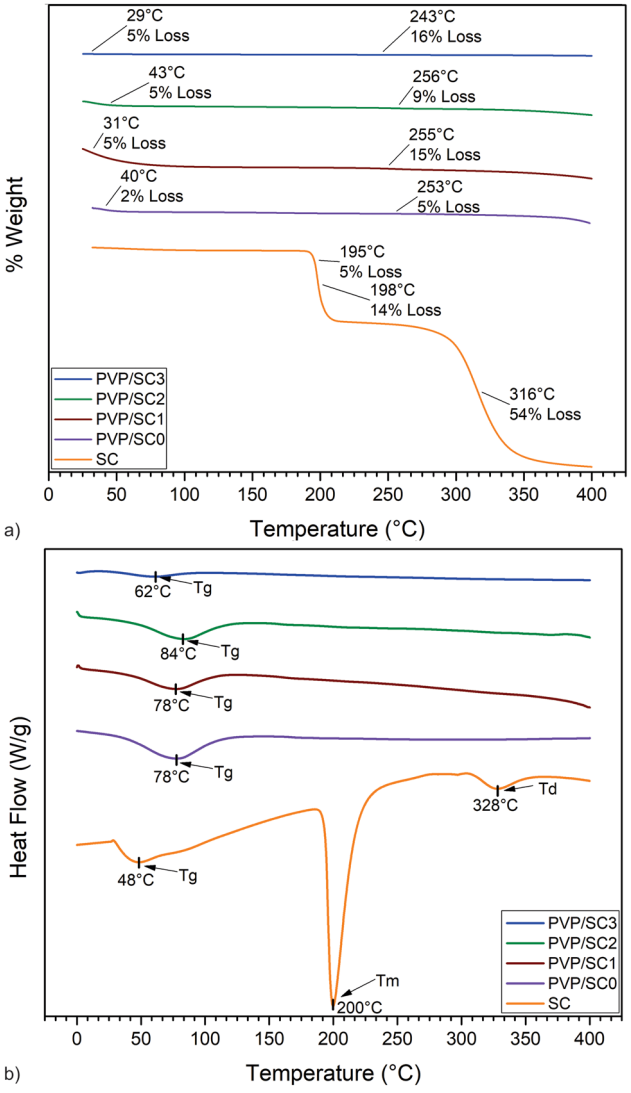

Figure 5: Thermal analysis of PVP/SC fibers. (a) TGA; (b) DSC.

of SC loaded increases on the fibers, a shift to slightly higher temperatures is observed (21). The T_m of SC, present in the loaded scaffolds, is not observed because of its low concentrations.

3.4 Wetting and dissolution rates

By exposing PVA/SC and PVP/SC scaffolds in distilled water, the effect of concentration of SC on wetting and dissolution times was analyzed to estimate their behavior in the oral cavity (22).

Video-recording in real-time conditions allowed measurements of wetting of scaffolds on water-wet paper at room temperature. Distilled water completely wet the PVA/SC1 and PVA/SC3 fibers in about 1 min, whereas in

PVA/SC2 wetting was almost instantaneous, being the most attractive of the PVA/SC scaffolds (see Figure 6a). Wetting of PVP/SC1 and PVP/SC3 fibers occurred in less than 5 s, whereas in PVP/SC2 wetting was faster (1.3 s), being the best attractive of this group (see Figure 6b).

Dissolution tests were performed by submerging the samples in a flask of distilled water at 37°C. The dissolution rate was also measured by video-recording in real time because it developed in seconds. First, water swelled the fibers forming transparent gel-like structures, while losing their white color. Then, disruption of the fiber structure occurred. PVA and PVA/SC fibers dissolved readily in the liquid medium, whereas PVP/SC fibers dispersed into hundreds of small pieces that spread through the medium very quickly, at 1.5 s approximately (23).

3.5 *In vitro* release analysis of SC

Table 3 shows the proportion of drug loaded in the nanofibers. After measuring all the samples, it was found that the distribution of the drug in the nanofiber scaffolds was homogeneous and loading is proportional to the concentration in the feeding solutions (24).

Also, SC presence was detected by UV-Vis spectroscopy, up to ~14% (3.5 mg) in the PVA fibers, and ~9% (2 mg) in the PVP fibers, but no significant difference (ANOVA $P < 0.05$) of SC loaded in the fibers was obtained.

Regarding drug release studies, the PVA/SC fibers had a burst release between 40% and 70% (PVA/SC1 and PVA/SC3 in respective order) in the first 30 s (see Figure 7), whereas PVP/SC fibers had a burst release of 100% in the same period, because all the samples were completely dissolved and released all SC in the first few

Table 3: Loaded SC concentration in PVA/SC and PVP/SC fibrous scaffolds

Samples	$\bar{x}$ (w/w%)	σ (%)
PVA/SC1	5.79	0.028
PVA/SC2	6.35	0.012
PVA/SC3	14.20	0.435
PVP/SC1	4.92	0.086
PVP/SC2	8.28	0.114
PVP/SC3	8.77	0.195

$\bar{x}$ = average; σ = standard deviation.

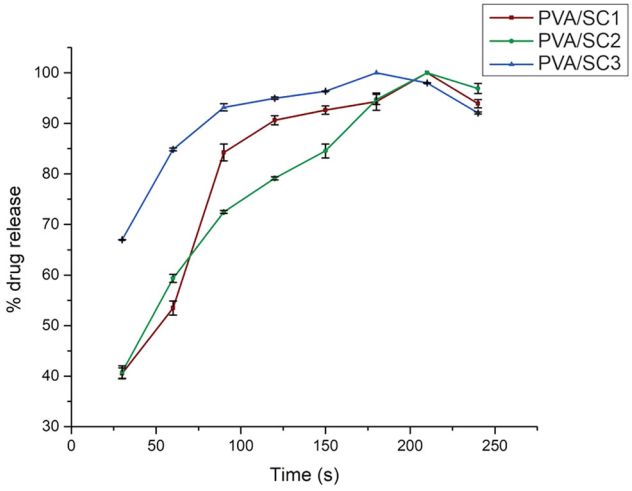

Figure 7: Release profile of SC in PVA/SC fibrous scaffolds.

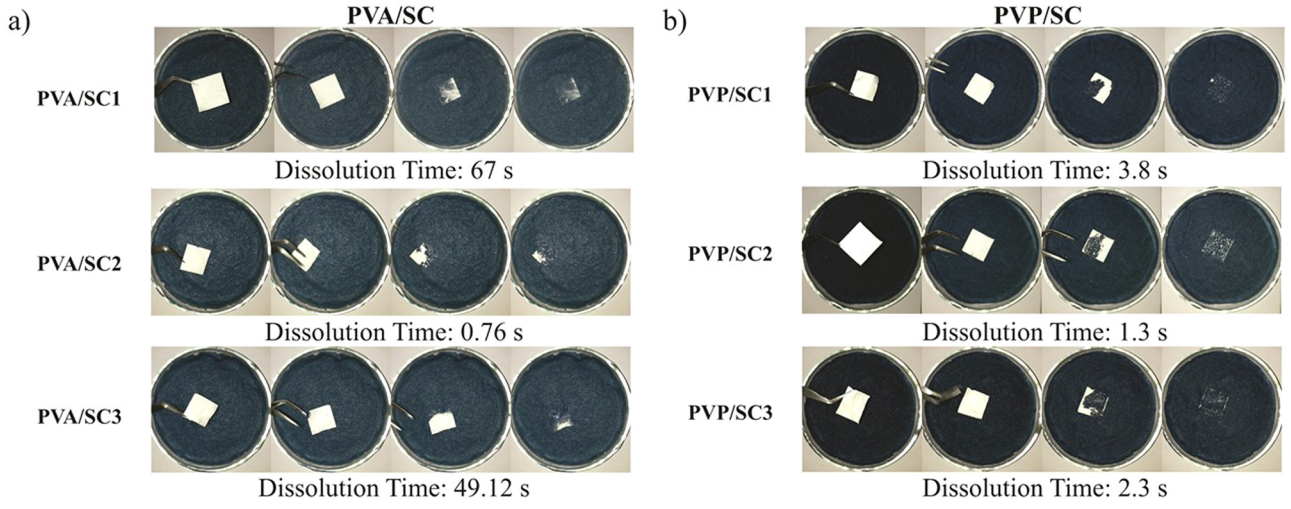

Figure 6: Wetting tests on the fibrous scaffolds: (a) PVA/SC fibers, (b) PVP/SC fibers.

seconds of immersion, making very difficult to register reliable release rate information (data not shown).

These results evidence the positive properties of the PVA/SC and PVP/SC scaffolds as SC drug release systems, i.e., high thermal stability, glass transitions ~45°C above room temperature, phase transitions above 200°C, quite short wetting and dissolution times, as well as proper SC release rates, suggesting convenient conditions for their potential use as controlled drug administration of SC for the treatment of PAH in children.

4 Discussion

FTIR spectra acquired for the pure polymer's nanofibers and the drug-loaded scaffolds are in agreement with those reported elsewhere. Drug incorporation into the nanofibers was shown by the presence of the carbonyl groups from the drug in the nanofibers of PVA/SC0 (24). Such analysis was not possible for the PVP/SC0 because of the overlapping of signals of the carbonyl groups present in the polymer and the drug.

Signals found in the PVA/SC0 fibers were according to literature (25). The presence of an intense peak at 3,400 cm^{-1} can be clearly seen. This peak is related to the stretching of O–H groups arising from the intramolecular and intermolecular hydrogen bonds. The peaks observed at 2,840 and 2,920 cm^{-1} are respectively related to the symmetric and antisymmetric stretching vibrational of C–H from alkyl groups (26). As reported by Coelho Neto and Lisboa (27), the characteristic signal of SC is the carbonyl group at ~1,695 cm^{-1}. This signal is evident in the PVA/SC spectra, confirming its incorporation (24).

In the case of PVP/SC0 fibers, signals showed that FTIR spectra were also consistent with literature (23). The characteristics peaks of PVP can be seen at 2,954, 1,654, 1,421, and 1,288 cm^{-1}, corresponding to the stretching vibrations of C–H, C–O, C–C, and C–N, respectively (23).

Electrospinning is a versatile technique for fabricating fibers with diameters in the order of nanometers to a few micrometers. This methodology has been proposed with great potential for preparing drug delivery systems and has recently received a great attention (28).

Chew et al. (29) confirmed that the release of bioactive molecules occurs primarily by diffusion, and it has been reported that the release profile of bioactive molecules from electrospun fibers can be influenced by biodegradability, fiber diameters, hydrophilicity, hydrophobicity, and fiber configuration.

For the electrospinning of the PVA/SC fibers, the nonionic surfactant TX-100 served to improve fiber formation (17). This is because of the difficulty of electrospinning of PVA at 20 kV of applied voltage, because according to calculations, 30 kV is the critical voltage when using DMF as a co-solvent (30). In addition, salts favor the electrospinning of polymers. Conveniently, SC is a salt that helped to promote high porosity and homogenous fibers, which is important to achieve high surface to volume ratio for fast dissolution. The combination of both factors, addition of TX-100 and loading a salt, produces fibers similar to that previously reported by Yao et al. (31).

Our PVP/SC fibers are similar in thickness to those reported in literature (16). The use of DMF as co-solvent allowed the efficient formation of submicron fibers (32). Notwithstanding the fact that drug concentration did not reached saturation, the highest concentration of SC worked in this study (5%) was the highest that permitted fiber formation in the electrospinning process (33).

For drug delivery applications, several fiber diameters have been described. For example, fibers with a core-shell of PVP/PCL for fast dissolving drug delivery, with a diameter less than 100 nm (34); PCL/cellulose nanocrystals with ~233 nm (35); and PCL/geranyl cinnamate with fibers in a range of 186.8 ± 6.2 nm (36) have been reported. In this work fibers are around ~400 nm, which are similar to the above-reported diameters. Nevertheless, Quan et al. (37) reported the preparation of fast-dissolving feruloyl-oleyl-glycerol-loaded PVP fibers with diameters of 700–800 nm, which are thicker than the ones in our study.

Thermal analysis is relevant for the study of drug delivery systems, as reported for several systems, including dendrimers, hydrogels, micelles, and nanoparticles (38), among others.

The TGA curves of the loaded nanofibers did not present loss of weight at ~198°C, as expected for the SC present in the fibers, suggesting strong hydrogen bonding between SC and PVA. This interaction is corroborated by DSC, because the T_m of SC shifts to a higher temperature and T_g's are displaced between all samples. It is worth noting that not all SC are bonding with the polymer, because two peaks are observed at ~185°C and ~208°C on DSC. The thermal properties of PVA have been previously reported (39). Silva Magalhães et al. (38) reported that the melting point of PVA scaffolds begins at approximately 200°C and thermal degradation initiates at about 239°C.

PVP is mostly an amorphous polymer that can undergo a transition phase that is related to vibrations

and segmental reptation movements of the polymer chains. In general, nanoscopic inclusions directly affect the behavior of polymeric nanocomposites, and the interaction of the polymer chains with the surface of the inclusion can significantly alter the chain kinetics of the region that is surrounded by these inclusions (39).

The data obtained in the TGA of PVP/SC0 show loss of weight, most probably from water adsorbed by the hygroscopic polymer (21,24). The polymer was stable at high temperatures (400°C), indicating that the polymer can be sterilized by strong heating, which is important for biomedical applications.

The DSC thermogram shows a shift in the T_g of the polymer, caused by the interaction between the polymer and the drug. By analyzing the higher temperature curves in the PVP/SC fibers, it can be noted that the characteristic peak of the SC (~200°C) disappears, indicating that the drug strongly interacts with PVP (24,29).

Nano and submicron fibers have both high surface free energy and high surface to volume ratio, which promote strong interactions with the surrounding media resulting, as is the case of PVA/SC and PVP/SC scaffolds, in fast dissolution rates of the fibers; for instance, nanofibers are a very good option for fast rate delivery systems (16).

In this study, PVA/SC fibers disintegrated in about 1–3 min. As it has been reported elsewhere, PVA fibers disintegrate easily and rapidly in aqueous solutions resulting in the fast release of drugs (24).

In the case of PVP scaffolds, these fibers improve the solubility of some hydrophobic drugs because PVP nanofibers help in their dispersion (40). Respect to our results, PVP/SC fibers show a very fast wetting and dissolving rates resulting in a very promising system for the ultra-rapid release of SC, for the sublingual administration of the drug.

Finally, maximum drug loading for successful electrospinning of the studied materials was 14% w/w (Table 3) because of the very low solubility of SC, in either water or ethanol. Nonetheless, the loaded nanofibers fulfill the criteria of very fast delivery systems, because all the loaded drugs were dissolved in about 3 min at 37°C in a suitable solvent (22).

PVA/SC fibers presented less burst release because PVA tends to swell in the presence of aqueous media, requiring up to 1 min for complete dissolution, whereas the PVP dissolves almost instantly releasing the drug in the first sampling time (30 s). As expected, the high surface area/volume ratio of the nanofibers facilitates the fast release of the SC in the media.

The aim of this study is to compare the two different SC nanocarriers, PVA- and PVP-loaded nanofibers, in terms of electrospinnability, drug loading efficiency, and drug release rates, to choose the best nanocarrier system for fast release of SC in the oral mucosa.

Different ratios of SC were loaded in the polymeric systems to evaluate the highest amount of SC that can be incorporated in the polymer solution to form the fibers. However, we observed that drug-loading reached a limit at 3.5 mg for a 25 mg sample of PVA/SC fibers mat (14% of SC) and 2 mg of SC for a 25 mg sample of PVP/SC fibers mat (9% of SC).

The maximum recommended dose of SC for children aged 1–17 years and weighing less than 20 kg is 10 mg, thrice a day (28). Therefore, the SC therapeutic dose in children (e.g., ~10 mg per sample) can be achieved by three 25 mg PVA/SC fibrous scaffold system (containing ~3.5 mg of SC) studied in the present work (~10.5 mg of SC). For practicality, the weight of the sample can be increased thrice to reach the desired doses. Nevertheless, the future goal of this project is to improve the SC loading for different controlled dosages in a 25 mg fibrous scaffold system.

Despite the aforementioned, PVP/SC system presented desired drug release rate (~2 s), with immediate dissolution when in contact with water. On the contrary, for PVA/SC it takes about ~49 s. In conclusion, both systems achieved fast release rate, being the PVP/SC system the best because of its faster dissolution rate and drug release.

Both PVA/SC and PVP/SC systems possess similar average fiber diameters (~417 nm vs ~411 nm). It is important to mention that the aim is to produce fibers with the lowest diameters possible, because this increases the surface area to volume ratio, enhancing drug load and drug dissolution rate (40).

Furthermore, both polymers have been reported to be biocompatible and both have been approved by FDA for drug delivery (24–26). Apart from all the properties discussed above, PVP/SC fibrous scaffolds have the extra advantage of faster drug release rate, compared to PVA/SC fibrous mats. Therefore, PVP/SC fibers are worthy to be further studied and optimized as a drug delivery system for SC.

Nowadays, work is underway to increase the loading of the drug in the fibers by complexation of SC by β-cyclodextrins, in an effort to reach SC therapeutic doses using smaller polymer weight (40).

5 Conclusion

Electrospinning is a technology for manufacturing continuous fiber scaffolds with a relatively simple configuration. However, in recent years, nano and submicron

electrospun fiber scaffolds have attracted much attention because of its potential applications in drug delivery systems. Its inherent high surface to volume ratio and cost-effectiveness are all attractive features for use in biomedical branches.

This study outlines the effect of the process parameters on the preparation of fibers loaded with SC, a drug used to treat PAH. PVA and PVP were electrospun with different proportions of the drug. As salts help the fiber formation, and SC is, conveniently, a salt, SC improved to some degree the electrospinning process.

The poor water solubility of the drug was solved by co-dissolving with DMF. Electrospinning was improved using a nonionic surfactant for PVA/SC fibers. It was noted that the PVA and PVP had a different behavior in their releasing profiles; while PVA/SC nanofibers had a complete SC release in about 1 min, PVP/SC nanofibers had a complete drug release in 4 s, making both polymers quite attractive for very fast drug delivery systems for the treatment of PAH in children.

The resulting loaded nanofibers present fast dissolution times that are adequate for the oral administrations of drugs. This system can be useful for the administration of SC to pediatric patients who otherwise have to be dosed with frequent syrup formulations, which is inconvenient for both the patients and the caregivers.

Acknowledgments: The authors thank the financial support of "Consejo Nacional de Ciencia y Tecnología (CONACYT)" for its grant known as "Fondo de Cooperación Internacional en Ciencia y Tecnología del Conacyt (FONCICYT)" in its grant named as "Convocatoria Conjunta de Movilidad 2015 CONACYT-DST México-India" with CONACYT project number 266380 and SICASPI-UABC number 351/375/E. The authors thank Universidad Nacional Autónoma de México for the support through the PAPIIT project IG100220 and to its technician QFB Karla Eriseth Reyes Morales for TGA and DSC analyses. The authors also thank the funding from the 20th Internal Call to Support Research Projects UABC. The authors thank Manuel A. Cornejo for the English proofreading of the manuscript.

Conflict of interest: The authors declare no conflicts of interest in this work.

References

(1) Sofianopoulou E, Church C, Coghlan G, Howard L, Johnson M, Kiely DG, et al. Deprivation and prognosis in patients with pulmonary arterial hypertension: Missing the effect of deprivation on a rare disease? Eur Respir J. 2020;56(2):1902334. doi: 10.1183/13993003.02334-2019.

(2) Bhogal S, Khraisha O, Al Madani M, Treece J, Baumrucker SJ, Paul TK. Sildenafil for pulmonary arterial hypertension. Am J Ther. 2019;26(4):e520–6. http://insights.ovid.com/crossref?an=00045391-201908000-00015.

(3) Cohen JL, Nees SN, Valencia GA, Rosenzweig EB, Krishnan US. Sildenafil use in children with pulmonary hypertension. J Pediatr. 2019 Feb;205:29–34.e1. doi: 10.1016/j.jpeds.2018.09.067.

(4) Beltrán-Gámez ME, Sandoval-Zárate J. Inhibidores de fosfodiesterasa-5 para el tratamiento de la hipertensión arterial pulmonar. Arch Cardiol Méx. 2015;85(3):215–24. doi: 10.1016/j.acmx.2015.03.001.

(5) Bartlett JA, van der Voort, Maarschalk K. Understanding the oral mucosal absorption and resulting clinical pharmacokinetics of asenapine. AAPS Pharm Sci Technol. 2012;13(4):1110–5. doi: 10.1208/s12249-012-9839-7.

(6) Villarreal-Gómez LJ, Serrano-Medina A, Torres-Martínez EJ, Perez-González GL, Cornejo-Bravo JM. Polymeric advanced delivery systems for antineoplasic drugs: Doxorubicin and 5-fluorouracil. E-Polym. 2018 Mar;18(4):359–72. doi: 10.1515/epoly-2017-0202

(7) Park J-C, Ito T, Kim K-O, Kim K-W, Kim B-S, Khil M-S, et al. Electrospun poly(vinyl alcohol) nanofibers: Effects of degree of hydrolysis and enhanced water stability. Polym J. 2010;42(3):273–6. doi: 10.1038/pj.2009.340%5Cn. http://www.nature.com/doifinder/10.1038/pj.2009.340

(8) Kadavil H, Zagho M, Elzatahry A, Altahtamouni T. Sputtering of electrospun polymer-based nanofibers for biomedical applications: A perspective. Nanomaterials (Basel). 2019 Jan. 8;9(1):77. doi: 10.3390/nano9010077.

(9) Chuangchote S, Sagawa T, Yoshikawa S. Electrospinning of poly(vinyl pyrrolidone): Effects of solvents on electrospinnability for the fabrication of poly(p-phenylene vinylene) and TiO_2 nanofibers. J Appl Polym Sci. 2009;114(5):2777–91. doi: 10.1002/app.30637.

(10) Marani D, Sudireddy BR, Nielsen L, Ndoni S, Kiebach R. Poly (vinyl pyrrolidone) as dispersing agent for cerium-gadolinium oxide (CGO) suspensions. J Mater Sci. 2016;51(2):1098–106. doi: 10.1007/s10853-015-9439-5.

(11) Li X, Kanjwal MA, Lin L, Chronakis IS. Electrospun poly vinyl-alcohol nanofibers as oral fast-dissolving delivery system of caffeine and riboflavin. Colloids Surf B Biointer. 2013;103:182–8. doi: 10.1016/j.colsurfb.2012.10.016.

(12) Pavia DL, Lampman GM, Kriz GS, Vyvyan JA. Introduction to Spectroscopy. 4th edn. Belmont, CA: Cengage; 2008.

(13) Wu H, Fan J, Chu CC, Wu J. Electrospinning of small diameter 3-D nanofibrous tubular scaffolds with controllable nanofiber orientations for vascular grafts. J Mater Sci Mater Med. 2010;21(12):3207–15. doi: 10.1007/s10856-010-4164-8.

(14) Araújo ES, Nascimento MLF, de Oliveira HP. Influence of triton X-100 on PVA fibres production by the electrospinning technique. Fibres Text East Eur. 2013;214(100):39–43. http://www.fibtex.lodz.pl/article949.html.

(15) Yu D-G, Shen X-X, Branford-White C, White K, Zhu L-M, Annie Bligh SW. Oral fast-dissolving drug delivery membranes prepared from electrospun poly vinylpyrrolidone ultrafine fibers.

Nanotechnology. 2009;20(5):055104. doi: 10.1088/0957-4484/20/5/055104.
(16) Torres-Martinez EJ, Cornejo Bravo JM, Serrano Medina A, Pérez González GL, Villarreal-Gómez LJ. A summary of electrospun nanofibers as drug delivery system: Drugs loaded and biopolymers used as matrices. Curr Drug Deliv. 2018;15(10):1360–74. doi: 10.2174/1567201815666180723114326.
(17) D'Avila Carvalho Erbetta C. Synthesis and characterization of poly(D,L-lactide-co-glycolide) copolymer. J Biomater Nanobiotechnol. 2012;3(2):208–25. doi: 10.4236/jbnb.2012.32027. http://www.scirp.org/journal/PaperDownload.aspx?.
(18) Guan Y, Shao L, Dong D, Wang F, Zhang Y, Wang Y. Bio-inspired natural polyphenol cross-linking poly(vinyl alcohol) films with strong integrated strength and toughness. RSC Adv. 2016;6:69966–72. doi: 10.1039/C6RA08904F.
(19) Patra N, Salerno M, Cernik M. Electrospun polyvinyl alcohol/pectin composite nanofibers. Electrospun Nanofibers. Sawston, Cambridge, London, United Kingdom: Elsevier Ltd; 2017. p. 599–608. doi: 10.1016/B978-0-08-100907-9.00022-2.
(20) Shahin HI, Vinjamuri BP, Mahmoud AA, Shamma RN, Mansour SM, Ammar HO, et al. Design and evaluation of novel inhalable sildenafil citrate spray-dried microparticles for pulmonary arterial hypertension. J Control Rel. 2019;302:126–39. doi: 10.1016/j.jconrel.2019.03.029.
(21) Veeren A, Bhaw-luximon A, Jhurry D. Poly vinyl pyrrolidone–poly caprolactone block copolymer micelles as nanocarriers of anti-TB drugs. Eur Polym J. 2013;49(10):3034–45. doi: 10.1016/j.eurpolymj.2013.06.020.
(22) Astha P, Prajal P. Detection of sildenafil citrate from aphrodisiac herbal formulations. Int J Pharm Sci Res. 2015;6(9):4080–5. doi: 10.1016/j.jpba.2009.05.021.
(23) Huang S, Zhou L, Li MC, Wu Q, Kojima Y, Zhou D. Preparation and properties of electrospun poly(vinyl pyrrolidone)/cellulose nanocrystal/silver nanoparticle composite fibers. Materials. 2016;9(7):E523. doi: 10.3390/ma9070523.
(24) Li X-Y, Wang X, Yu D-G, Ye S, Kuang Q-K, Yi Q-W, et al. Electrospun Borneol-PVP nanocomposites. J Nanomater. 2012;2012:1–8. doi: 10.1155/2012/731382.
(25) Sabzi M, Afshari MJ, Babaahmadi M, Shafagh N. pH-dependent swelling and antibiotic release from citric acid cross-linked poly(vinyl alcohol) (PVA)/nano silver hydrogels. Colloids Surf B Biointer. 2020;188:110757. doi: 10.1016/j.colsurfb.2019.110757.
(26) Awada H, Daneault C. Chemical modification of poly(vinyl alcohol) in water. Appl Sci. 2015;5:840–50. doi: 10.3390/app5040840.
(27) Coelho Neto J, Lisboa FLC. ATR-FTIR characterization of generic brand-named and counterfeit sildenafil- and tadalafil-based tablets found on the Brazilian market. Sci Justice. 2017;57(4):283–95. doi: 10.1016/j.scijus.2017.04.009.
(28) Villarreal-Gómez LJ, Vera-Graziano R, Vega-Rios MR, Pineda-Camacho JL, Mier-Maldonado PA, Almanza-Reyes H, et al. Biocompatibility evaluation of electrospun scaffolds of poly(L-lactide) with pure and grafted hydroxyapatite. J Mex Chem Soc. 2014;58:435–43.
(29) Chew S, Wen J, Yim E, Leong K. Sustained release of proteins from electrospun biodegradable fibers. Biomacromolecules. 2005;6(4):2017–24. doi: 10.1021/bm0501149.
(30) Bai J, Li Y, Yang S, Du J, Wang S, Zheng J, et al. A simple and effective route for the preparation of poly(vinylalcohol) (PVA) nanofibers containing gold nanoparticles by electrospinning method. Solid State Commun. 2007;141(5):292–5. http://linkinghub.elsevier.com/retrieve/pii/S0038109806009446.
(31) Yao L, Haas TW, Guiseppi-Elie A, Bowlin GL, Simpson DG, Wnek GE. Electrospinning and stabilization of fully hydrolyzed poly(vinyl alcohol) fibers. Chem Mater. 2003;15(9):1860–4. doi: 10.1021/cm0210795.
(32) Ramis J, Pajarito B. New solvent system for the fabrication of poly vinyl alcohol – gelatin nanofibers via electrospinning. Adv Mater Res. 2015;1125:406–10. http://www.scientific.net/AMR.1125.406.
(33) Dhariwal AK, Bavdekar SB. Sildenafil in pediatric pulmonary arterial hypertension. J Postgrad Med. 2015;61(3):181–92. doi: 10.4103/0022-3859.159421.
(34) Li JJ, Yang YY, Yu DG, Du Q, Yang XL. Fast dissolving drug delivery membrane based on the ultra-thin shell of electrospun core-shell nanofibers. Eur J Pharm Sci. 2018;122:195–204. doi: 10.1016/j.ejps.2018.07.002.
(35) Hivechi A, Bahrami SH, Siegel RA. Drug release and biodegradability of electrospun cellulose nanocrystal reinforced polycaprolactone. Mater Sci Eng C. 2019;94:929–37. doi: 10.1016/j.msec.2018.10.037.
(36) McInnes SJ, Macdonald TJ, Parkin IPP, Nann T, Voelcker NH. Electrospun composites of polycaprolactone and porous silicon nanoparticles for the tunable delivery of small therapeutic molecules. Nanomaterials. 2018;8:205. doi: 10.3390/nano8040205.
(37) Quan J, Yu Y, Branford-White C, Williams GR, Yu DG, Nie W, et al. Preparation of ultrafine fast-dissolving feruloyl-oleylglycerol-loaded polyvinylpyrrolidone fiber mats via electrospinning. Colloids Surf B Biointerfaces. 2011;88(1):304–9. doi: 10.1016/j.colsurfb.2011.07.006.
(38) Silva Magalhães M, Toledo RD, Fairbairn EMR. Durability under thermal loads of polyvinyl alcohol fibers. Matéria. 2013;18(4):1587–95. doi: 10.1590/S1517-70762013000400018.
(39) Aqeel SM, Al-Shuja'a O, Huang Z, Le C, Zhang Y, Wang Z. Improved thermal and electrical properties of nanocomposites based on poly(vinyl pyrrolidone)/poly(acrylonitrile)/multi-walled carbon nanotubes. J Chem Eng Chem Res. 2015;2(9):771–9. https://www.ncbi.nlm.nih.gov/pmc/articles/PMC5796563/.
(40) Torres-Martinez EJ, Pérez-González GL, Serrano-Medina A, Grande D, Vera-Graziano R, Cornejo-Bravo JM, et al. Drugs loaded into electrospun polymeric nanofibers for delivery. J Pharm Pharm Sci. 2019;22(1):313–31. doi: 10.18433/jpps29674.